

RUBIDIUM ABUNDANCES IN THE GLOBULAR CLUSTERS NGC 6752, NGC 1904 AND NGC 104 (47 TUC)<sup>1</sup>VALENTINA D'ORAZI<sup>2,3</sup>, MARIA LUGARO<sup>3</sup>, SIMON W. CAMPBELL<sup>3</sup>, ANGELA BRAGAGLIA<sup>4</sup>, EUGENIO CARRETTA<sup>4</sup>, RAFFAELE G. GRATTON<sup>5</sup>, SARA LUCATELLO<sup>5</sup>, AND FRANCESCA D'ANTONA<sup>6</sup>

## ABSTRACT

Large star-to-star variations of the abundances of proton-capture elements, such as Na and O, in globular clusters (GCs) are interpreted as the effect of internal pollution resulting from the presence of multiple stellar populations. To better constrain this scenario we investigate the abundance distribution of the heavy element rubidium (Rb) in NGC 6752, NGC 1904, and NGC 104 (47 Tuc). Combining the results from our sample with those in the literature, we found that Rb exhibits no star-to-star variations, regardless the cluster metallicity, with the possible intriguing, though very uncertain, exception of the metal-rich bulge cluster NGC 6388. If no star-to-star variations will be confirmed for all GCs, it implies that the stellar source of the proton-capture element variations must not have produced significant amounts of Rb. This element is observed to be enhanced at extremely high levels in intermediate-mass AGB (IM-AGB) stars in the Magellanic Clouds (i.e., at a metallicity similar to 47 Tuc and NGC 6388). This may present a challenge to this popular candidate polluter, unless the mass range of the observed IM-AGB stars does not participate in the formation of the second-generation stars in GCs. A number of possible solutions are available to resolve this conundrum, also given that the Magellanic Clouds observations are very uncertain and may need to be revised. The fast rotating massive stars scenario would not face this potential problem as the slow mechanical winds of these stars during their main-sequence phase do not carry any Rb enhancements; however, these candidates face even bigger issues such as the production of Li and the close over-imposition with core-collapse supernova timescales. Observations of Sr, Rb, and Zr in metal-rich clusters such as NGC 6388 and NGC 6441 are sorely needed to clarify the situation.

*Subject headings:* stars: abundances —stars: Population II —stars: AGB and post-AGB —globular clusters: individual (NGC 1904, NGC 6752, NGC 104)

## 1. INTRODUCTION

It is now well established that Galactic globular clusters (GCs) host multiple stellar populations. This is evidenced by large star-to-star variations in elements affected by proton captures (Na, O, Mg, Al, hereafter p-capture elements, e.g., Cohen 1999; Ivans et al. 1999; Marino et al. 2008; Carretta et al. 2010), and in some cases by the splitting of the evolutionary sequences in colour-magnitude diagrams (e.g., Anderson et al. 2009; Piotto 2009; Monelli et al. 2013; Milone et al. 2013). The most popular explanation for the existence of multiple populations is the internal pollution scenario, which relies on the occurrence of at least two different episodes of star formation. In this picture a portion of the first-generation stars (FG, O/Mg/C-rich and Na/Al/N-poor) underwent nucleosynthesis through the proton capture (CNO, NeNa, and possibly MgAl) cycles and polluted the interstellar medium with the processed material via stellar winds. The second stellar generation (SG, O/Mg/C-poor and Na/Al/N-rich) formed from this enriched material, probably within about one hundred Myr (see Ventura & D'Antona 2009 and

Gratton et al. 2012 for a review).

Observational data from high-resolution spectroscopy and accurate photometric surveys are starting to provide substantial constraints on the internal pollution scenario. Currently the debate centres around the fundamental but as yet unanswered question: *which of the FG stars were the polluters?* The candidates are necessarily the more massive, short-lived FG stars that existed early in the GC evolution, although they could not have been supernovae because the Ca and Fe-group content is observed to be constant (with a few peculiarities such as, e.g.,  $\omega$  Cen, M22, NGC 1851, see, e.g., Marino et al. 2009, Carretta et al. 2011; Yong & Grundahl 2008) and their fast ejecta cannot be retained in GCs. The main competitors include intermediate-mass asymptotic giant branch stars (IM-AGB; Ventura et al. 2001; Ventura & D'Antona 2009), Super-AGB stars (Ventura & D'Antona 2011; D'Ercole et al. 2012), and fast rotating massive stars (FRMS; Decressin et al. 2007), with novae (Maccarone & Zurek 2012) and massive binaries (de Mink et al. 2009) also being suggested.

Apart from the lack of consensus on the stellar source of the pollution, there are also many other open issues relating to the chemical abundance differences within GCs. For example, it is presently unclear whether the p-capture element distributions show continuous or discrete behaviour (e.g., Marino et al. 2008; Carretta et al. 2013), and if these distributions have a possible connection with the cluster structural parameters (e.g., mass, metallicity, horizontal branch morphology, see, e.g., Gratton et al. 2011; Bragaglia et al. 2012). Due to these ambiguities several observational studies have explored other elements, with a view to providing better constraints for the theoretical models. This has been done for Li and F (e.g., Pasquini et al. 2005; D'Orazi & Marino 2010; Shen et al. 2010; Lind et al. 2011; Mucciarelli et al. 2011;

valentina.dorazi@mq.edu.au

<sup>1</sup> Based on observations taken with ESO telescopes under program 085.D-0205(A)

<sup>2</sup> Department of Physics and Astronomy, Macquarie University, Balaclava Rd, North Ryde, NSW 2109, Australia

<sup>3</sup> Monash Centre for Astrophysics, Monash University, School of Mathematical Sciences, Building 28, Clayton, VIC 3800, Australia

<sup>4</sup> INAF Osservatorio Astronomico di Bologna, via Ranzani 1, I-40127 Bologna, Italy

<sup>5</sup> INAF Osservatorio Astronomico di Padova, vicolo dell'Osservatorio 5, I-35122 Padova, Italy

<sup>6</sup> INAF Osservatorio Astronomico di Roma, via Frascati 33, I-00040 Monteporzio, Italy

Smith et al. 2005; Yong et al. 2008c; Alves-Brito et al. 2012; D'Orazi et al. 2013b; de Laverny & Recio-Blanco 2013) and for trans-iron elements produced by *slow* neutron captures (the *s*-process, e.g., Armosky et al. 1994; James et al. 2004; Smith 2008). These previous works have shown that *s*-process element abundances display a homogeneous abundance pattern in the majority of GCs (see also D'Orazi et al. 2010 who derived the Ba content for a sample of more than 1000 stars in 15 Galactic GCs). Interestingly, the picture is further complicated by the presence of some exceptions: in M22 Marino et al. (2009) measured a variation in the *s*-process elements Y, Zr, and Ba correlated with a metallicity change, in NGC 1851 Ba has been found to vary from a factor of four to more than one dex (Yong & Grundahl 2008; Villanova et al. 2010; Carretta et al. 2011), and in the most spectacular case of  $\omega$  Centauri an increasing trend of Ba and La as a function of [Fe/H] has been revealed by the comprehensive high-resolution spectroscopic surveys of Johnson & Pilachowski (2010) and Marino et al. (2011a).

In the current study we focus on rubidium (Rb), an element of mixed *s*-process and *rapid* neutron capture (*r*-process) origin (Arlandini et al. 1999; Goriely 1999). The production of Rb during the *s*-process is controlled by the neutron density. If the neutron density reaches higher than  $\sim 10^9$  n/cm<sup>3</sup>, the *s*-process can proceed through <sup>87</sup>Rb instead of <sup>85</sup>Rb via neutron captures on <sup>85</sup>Kr and <sup>86</sup>Rb, two unstable isotopes with half-lives against  $\beta$  decay long enough to represent “branching points” on the path of neutron captures. Because <sup>87</sup>Rb has a magic number of neutrons, its neutron-capture cross section is more than an order of magnitude smaller than that of <sup>85</sup>Rb (Heil et al. 2008). This results in an enhanced production of Rb with respect to neighbouring *s*-process elements, such as Sr and Zr, which are not affected by the operation of branching points. Due to this property of the Rb production, the [Rb/Sr] (or [Rb/Zr]) ratio spectroscopically observed in AGB stars has been used to derive the neutron density during the *s*-process, from which the neutron source and the initial stellar mass can be inferred (Busso et al. 1995; Abia et al. 2001; García-Hernández et al. 2006; van Raai et al. 2012). AGB stars are well known to be the main source of *s*-process elements in the Galaxy. In the standard picture, two neutron sources are present in the He-rich shell of AGB stars (Gallino et al. 1998). The <sup>13</sup>C( $\alpha$ ,n)<sup>16</sup>O reaction is activated in low-mass (< 4 M<sub>⊙</sub>) AGB stars in radiative conditions and produces low neutron densities ( $\sim 10^8$  n/cm<sup>3</sup>), resulting in negative [Rb/Sr] and [Rb/Zr] ratios<sup>7</sup>. The <sup>22</sup>Ne( $\alpha$ ,n)<sup>25</sup>Mg reaction is activated in the convective thermal pulses of IM-AGB stars and produces high neutron densities (up to  $\sim 10^{13}$  n/cm<sup>3</sup>), resulting in positive [Rb/Sr] and [Rb/Zr] ratios. These positive ratios are a critical, possibly unique, signature of the *s*-process in IM-AGB stars (van Raai et al. 2012; Karakas et al. 2012).

Also FRMS are predicted by theoretical models to efficiently activate the <sup>22</sup>Ne( $\alpha$ ,n)<sup>25</sup>Mg reaction resulting in the production of *s*-process elements (Pignatari et al. 2008; Frischknecht et al. 2012). However, these stars do not experience neutron densities as high as IM-AGB stars, and produce negative [Rb/Sr] and [Rb/Zr] ratios<sup>1</sup> (see Figure 1 of Frischknecht et al. 2012). Furthermore, the *s*-process elements are produced in the late evolutionary phases of FRMS

and ejected in the interstellar medium during the core-collapse supernova explosion. The FRMS scenario of GCs, on the other hand, involves pollution from the winds of these stars, which occur previous to the explosion. This is required both to allow the material to remain in the GCs, as the supernova fast ejecta are not retained by GCs (with the exception of the most massive GCs, e.g.,  $\omega$  Centauri), and to avoid variations in Fe. In summary, the FRMS winds carry variations in proton-capture elements but not in the *s*-process elements.

Clearly, observational information on the *s*-process elements, and Rb in particular, in GCs is crucial to be compared to theoretical models of the potential stellar sources of pollution. To date Rb abundances have been reported only for a handful of GCs: NGC 6752 (Yong et al. 2006), NGC 6388 (Wallerstein et al. 2007), M4 and M5 (Yong et al. 2008b; D'Orazi et al. 2013a),  $\omega$  Centauri (Smith et al. 2000), and NGC 3201 (Gonzalez & Wallerstein 1998). In this paper we extend upon the previous investigations and present Rb abundances in two more GCs: NGC 1904 and 47 Tuc ([Fe/H]=−1.60 dex and [Fe/H]=−0.72 dex, respectively, Harris 1996-update in 2010). Furthermore, we report Rb abundances for another 6 giant stars in NGC 6752 ([Fe/H]=−1.54), complementing the previous work by Yong et al. (2006). The information derived from metal-rich GCs such as NGC 6388 and 47 Tuc is crucial because not only it provides us with Rb abundances for a large range of GC metallicities – covering  $\sim 1$  dex – but also it allows us to make a direct comparison with recent Rb measurements in IM-AGB stars of similar metallicity in the Magellanic Clouds (García-Hernández et al. 2009).

Abundances of other *s*-process elements in the three GCs considered here have been analysed by several groups. François (1991) analysed the Ba content for four giant stars in NGC 1904, finding a mean value of [Ba/Fe]=0.08±0.08, while D'Orazi et al. (2010) presented the Ba abundances for a sample of 49 giants, reporting a constant value of [Ba/Fe]=0.24±0.03. NGC 6752 has been previously studied by several authors including James et al. (2004), who found [Sr/Fe]=0.06±0.07, [Y/Fe]=−0.02±0.01, [Ba/Fe]=0.18±0.07 for nine sub-giant and nine turn-off stars, and Yong et al. (2005), who analysed a sample of 38 giants in NGC 6752 and derived mean values of [Y/Fe]=−0.02±0.01, [Zr/Fe]=+0.18±0.02, [Ba/Fe]=−0.06±0.02, [La/Fe]=0.10±0.01, and [Ce/Fe]=0.27±0.01. Finally, *s*-process element abundance in the metal-rich GC 47 Tuc were published by James et al. (2004, [Sr/Fe]=0.32±0.04, [Y/Fe]=−0.03±0.09, [Ba/Fe]=0.29±0.07); Alves-Brito et al. (2005, [Ba/Fe]=0.35±0.05, [La/Fe]=0.05±0.05); D'Orazi et al. (2010, [Ba/Fe]=0.15±0.01), and Worley et al. (2010, [Y/Fe]=0.50±0.04, [Zr/Fe]=0.49±0.03, [Ba/Fe]=0.34±0.13, [La/Fe]=0.32±0.03). In summary, all these previous investigations have shown that in these three GCs the extremely large variations exhibited in the p-capture elements (Na, O, Mg, Al) are not displayed by any *s*-process elements. With the present study we extend these previous investigations in relation to the crucial element Rb.

## 2. STELLAR SAMPLE, OBSERVATIONS, AND ANALYSIS

We analysed a sample of 15 RGB stars (six in NGC 6752, five in NGC 1904, and four in 47 Tuc) whose stellar parameters and p-capture element abundances have been published by Carretta et al. (2007, 2009). The clusters under consideration span a large range in metallicity ( $-1.5 \lesssim [\text{Fe}/\text{H}]$

<sup>7</sup> The [Rb/Zr] ratio may be positive in the specific case of a neutron exposure so low to not allow the flux to bypass the very first bottleneck on the *s*-process path at the magic nucleus <sup>88</sup>Sr.

$\lesssim -0.7$  dex), absolute visual magnitude (a proxy for the current mass), horizontal branch morphology, and range/shape of the light-element anti-correlations (Carretta et al. 2010). Within each GC we targeted both FG (O-rich/Na-poor) and SG (O-poor/Na-rich) stars, covering almost the whole extent of the Na-O anti-correlations (see Carretta et al. 2009b).

High-resolution spectra were acquired with FLAMES-UVES (R=47,000; Pasquini et al. 2002), employing the standard setup at 860 nm (spectral coverage  $\lambda\lambda 6600 \text{ \AA} - 10600 \text{ \AA}$ ), which includes the Rb I resonance line at  $\lambda=7800.268 \text{ \AA}$ . data reduction has been accomplished by the ESO personnel for NGC 1904 and NGC 6752 targets, while we performed data reduction for 47 Tuc by means of the ESO FLAMES-UVES pipeline (version 5.1.0<sup>8</sup>), running under GASGANO context, and following the standard procedure (bias subtraction, flat-field correction, optimal extraction, and wavelength calibration). The output one-dimensional spectra were then sky subtracted, shifted to zero radial velocity and continuum normalised within IRAF<sup>9</sup>. The typical S/N ratios are in the range 80-150 per pixel at  $\sim 7800 \text{ \AA}$ .

Rb abundances were determined via spectral synthesis with MOOG (Snedden 1973, 2011 version) and the Kurucz (1993) grid of model atmospheres, with the overshooting option switched on, consistently with Carretta et al. (2009b). We note that this choice has negligible impact on our derived Rb abundances. The spectral line broadening, assumed to be Gaussian, was evaluated by fitting the profile of the Ni I line at  $\lambda=7797.59 \text{ \AA}$ .

We then computed synthetic spectra varying the abundances of Rb until the best match with the observed spectrum was achieved. The high excitation Si I feature at  $\lambda=7799 \text{ \AA}$  partially blends the Rb line on its left wing. We initially assumed (when available) the [Si/Fe] ratios derived by Carretta et al. (2007, 2009a) and then optimised those values to better reproduce the line under scrutiny here. The agreement between the [Si/Fe] ratios derived by us and by Carretta et al. is always within 0.05 dex. By considering the typical uncertainty reported by Carretta and collaborators for their Si abundances, we evaluated the impact of the [Si/Fe] on Rb abundances being in the range 0.04 - 0.09 dex (depending on the GC and on the star).

Examples of the spectral synthesis are shown in Figure 1 where we present three stars from our sample, each from a different GC. The spectral region around the Rb resonance line at  $7800 \text{ \AA}$  is contaminated by the presence of several weak CN lines; however, their inclusion has negligible impact on the derived Rb abundances, as also discussed in detail by Yong et al. (2008b) and D’Orazi et al. (2013a). We employed the same linelist as D’Orazi et al. (2013a) who used wavelength shifts and hyperfine structure components from Lambert & Luck (1976) and assumed the isotopic ratio  $^{85}\text{Rb}/^{87}\text{Rb} = 3$  (Tomkin & Lambert 1999). We note that the activation of the s-process branching points at  $^{85}\text{Kr}$  and  $^{86}\text{Rb}$  responsible for enhancing the Rb production in IM-AGB stars is also known to produce  $^{85}\text{Rb}/^{87}\text{Rb}$  ratios less than 3. For [Rb/Fe]  $\sim 1.5$  the ratio reduces to  $\sim 0.3$  (Table 3 of van Raai et al. 2012). We tested the effect that of this lower

limit has on the spectral synthesis and found that the [Rb/Fe] ratio increases by only  $\sim +0.2$  dex, which is similar to the measurement uncertainties. We refer to D’Orazi et al. (2013a) study for further details on the atomic oscillator strengths and the abundances for the Sun and Arcturus. In Figure 2 we show the [Rb/Fe] ratios for all our sample stars as a function of the stellar parameters ( $T_{\text{eff}}$ ,  $\log g$ , and microturbulence  $\xi$ ). For NGC 1904, due to relatively warmer temperatures of the target stars (see Table 1), we could derive the Rb abundance only for one star (#98). For the other four stars upper limits are given.

Random uncertainties related to best-fit determinations and to the adopted stellar parameters affect the abundances derived through spectral synthesis. We found errors in the best-fit procedure (reflecting the S/N of the spectra and the continuum placement) to be  $\sim 0.05$  dex (in [Rb/Fe]) for 47 Tuc and  $\sim 0.10$  dex for NGC 6752 and NGC 1904. The sensitivity of [Rb/Fe] to the input atmospheric parameters was evaluated in the standard way, i.e., changing a parameter at the time and inspecting the corresponding variation in the resulting abundance. We assumed variations of  $\Delta T_{\text{eff}} = \pm 50 \text{ K}$ ,  $\Delta \log g = \pm 0.2$  dex,  $\Delta \xi = \pm 0.1 \text{ km s}^{-1}$ , and  $\Delta [A/H] = \pm 0.1$  dex (Table 2); we then computed uncertainties relating to the stellar parameters adopting errors given by Carretta et al. (2009b) for NGC 1904 and 47 Tuc (error values as reported in their Table A2 are:  $T_{\text{eff}}=6\text{K}$ ,  $\log g=0.04$ ,  $[A/H]=0.03$ ,  $\xi=0.11 \text{ km s}^{-1}$  for 47 Tuc and  $T_{\text{eff}}=5\text{K}$ ,  $\log g=0.04$ ,  $[A/H]=0.03$ ,  $\xi=0.20 \text{ km s}^{-1}$  for NGC 1904) and by Carretta et al. (2007) for NGC 6752 (errors are  $T_{\text{eff}}=5\text{K}$ ,  $\log g=0.05$ ,  $[A/H]=0.05$ ,  $\xi=0.13 \text{ km s}^{-1}$ ). The typical total uncertainties in [Rb/Fe] due to stellar parameters range between 0.03–0.05 dex.

### 3. RESULTS

In Table 1 we present our resulting Rb (and Si) abundances, along with the stellar parameters and Fe, Na, and O abundances by Carretta et al. (2007, 2009).

In NGC 6752 we find the mean Rb abundance to be [Rb/Fe] =  $-0.08 \pm 0.02$  (rms = 0.04). This compares well with the value of [Rb/Fe] =  $-0.17 \pm 0.06$  reported by Yong et al. (2006), implying a difference of  $0.09 \pm 0.06$  dex. The small divergence, which is within the measurement errors (Section 2), is probably due to differences in temperature and/or metallicity scales: our [Fe/H] ratios are on average slightly higher and the stars in the sample of Yong et al. (2006) are cooler than those analysed here; unfortunately we cannot make a direct comparison because none of our sample stars is in common with that study. Based on their findings, Yong et al. (2006) noted that the Rb abundances in NGC 6752 appear to be concentrated around two distinct values, with two stars exhibiting [Rb/Fe]  $\approx -0.02$  and the other three stars [Rb/Fe]  $\approx -0.25$ . However, although there was a (possibly bimodal) spread in the Rb data of Yong et al. (2006), they concluded that it is unlikely NGC 6752 displays a real dispersion because the uncertainties arising from the weakness of the Rb I line were quite large. Most importantly, they found no correlation between [Rb/Fe] and p-capture elements known to vary considerably in GCs. Our results deliver further support to this previous

<sup>8</sup> Available at <http://www.eso.org/sci/software/pipelines/>

<sup>9</sup> IRAF (Image Reduction and Analysis Facility) is distributed by the National Optical Astronomy Observatories, which are operated by the Association of Universities for Research in Astronomy, Inc., under cooperative agreement with the National Science Foundation.

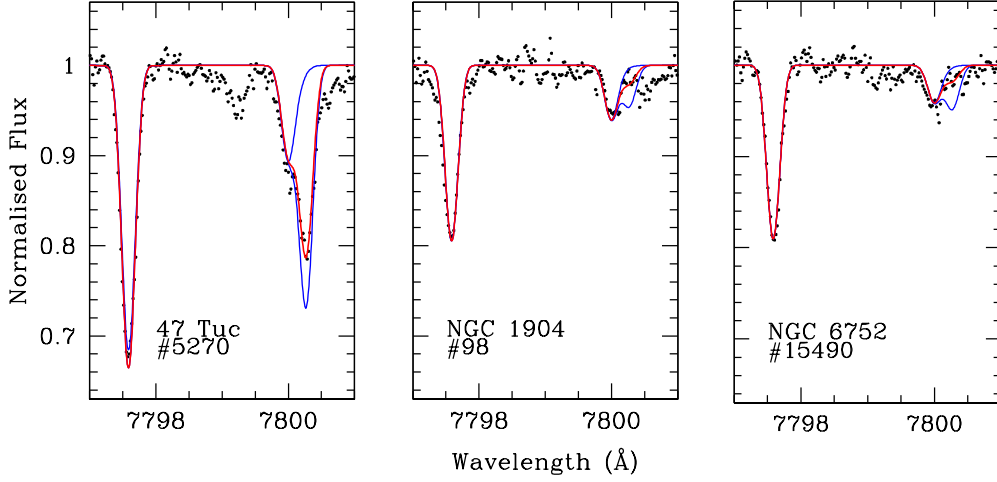


FIG. 1.— Example of the spectral synthesis for star #5270 (47 Tuc), #98 (NGC 1904), and #15499 (NGC 6752). Different syntheses are for  $A(\text{Rb i})=\text{none}$ , best-fit and best-fit+0.3 dex values.

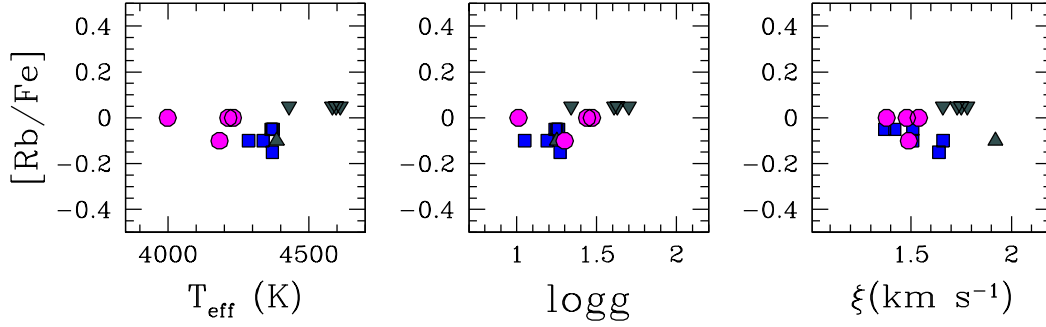


FIG. 2.— Rb abundances as a function of the effective temperature, gravity, and microturbulence for our sample stars. Squares, triangles, and circles are for NGC 6752, NGC 1904, and 47 Tuc, respectively. Upside-down triangles represent upper limits.

TABLE 1

STELLAR PARAMETERS (FROM CARRETTA ET AL. 2007, 2009B) AND ABUNDANCES (NA AND O FROM CARRETTA ET AL. 2007, 2009B, SI AND RB FROM THE PRESENT STUDY).

Star	$T_{\text{eff}}$ (K)	$\log g$ (dex)	$\xi$ ( $\text{km s}^{-1}$ )	[Fe/H] (dex)	[O/Fe] (dex)	[Na/Fe] (dex)	[Si/Fe] (dex)	[Rb/Fe] (dex)
NGC 6752 7627	4373	1.26	1.42	-1.53	-0.08	0.72	0.45	-0.05
NGC 6752 9756	4369	1.25	1.51	-1.59	0.47	0.04	0.47	-0.05
NGC 6752 15590	4366	1.24	1.37	-1.46	-0.12	0.74	0.50	-0.05
NGC 6752 23999	4286	1.05	1.51	-1.56	0.02	0.55	0.48	-0.10
NGC 6752 15490	4338	1.19	1.66	-1.55	0.42	0.13	0.40	-0.10
NGC 6752 21828	4371	1.27	1.64	-1.51	0.38	0.30	0.40	-0.15
NGC 1904 113	4430	1.34	1.66	-1.54	-0.50	0.55	0.30	<0.05
NGC 1904 185	4596	1.63	1.73	-1.55	0.09	0.61	0.30	<0.05
NGC 1904 181	4583	1.61	1.78	-1.55	.....	0.63	0.35	<0.05
NGC 1904 193	4612	1.70	1.75	-1.57	0.32	0.15	0.30	<0.05
NGC 1904 98	4386	1.25	1.92	-1.57	0.36	-0.05	0.32	-0.10
47 Tuc 13795	4183	1.30	1.49	-0.83	0.36	0.30	0.45	-0.10
47 Tuc 14583	4231	1.47	1.54	-0.68	0.34	0.43	0.40	0.00
47 Tuc 23821	4214	1.44	1.38	-0.78	0.39	0.44	0.37	0.00
47 Tuc 5270	3999	1.01	1.48	-0.77	0.12	0.69	0.45	0.00

TABLE 2  
[Rb/Fe] DEPENDENCY ON MODEL PARAMETERS FOR TWO OF OUR STARS

	$T_{\text{eff}}+50$	$\log g+0.2$	$\xi+0.1$	$[A/H]+0.1$
$\Delta[\text{Rb}/\text{Fe}]_{\#5270}$	0.06	-0.03	-0.02	-0.07
$\Delta[\text{Rb}/\text{Fe}]_{\#15490}$	0.04	-0.02	-0.02	-0.08

work, confirming the lack of an internal spread in Rb abundances for NGC 6752. This abundance pattern is in agreement with other heavy-element abundances, such as the second-peak element Ba investigated by D’Orazi et al. (2010) and the third-peak element Pb analysed by Yong et al. (2006), who concluded that neither elements exhibit any intrinsic spread in this cluster. Yong et al. (2005) determined abundances for a sample of 38 NGC 6752 giants and found a small variation in the light  $s$ -process Y and Zr and in the heavy  $s$ -process Ba, positively correlated with the Al variation. However, the detected enhancement in the  $s$ -process elements is at roughly the same level of the measurement uncertainties and, if real, might imply a quite peculiar chemical pattern, since according to our data and those of Yong et al. (2006), Rb does not display the same kind of internal variation. It could be, however, that the relatively large uncertainties (see also discussion in Yong et al. 2006) in the Rb abundances prevent us from identifying a change in its content at the  $\sim 0.1$  dex level.

Because of the relatively warmer temperatures of our stars, only one Rb measurement was possible for NGC 1904:  $[\text{Rb}/\text{Fe}] = -0.10 \pm 0.12$  dex for star #98, while upper limits are provided for the other giants. The value obtained for star #98 is very close to the average Rb abundance in NGC 6752. These two GCs also share an almost identical metallicity and Ba abundance:  $[\text{Ba}/\text{Fe}] = 0.28 \pm 0.02$  and  $[\text{Ba}/\text{Fe}] = 0.24 \pm 0.03$  for NGC 6752 and NGC 1904, respectively (D’Orazi et al. 2010).

Finally, for the metal-rich GC 47 Tuc we found a mean abundance of  $[\text{Rb}/\text{Fe}] = -0.03 \pm 0.03$  (rms = 0.05), i.e., a solar  $[\text{Rb}/\text{Fe}]$  ratio and no evidence of internal scatter.<sup>10</sup>

Figure 3 displays  $[\text{Rb}/\text{Fe}]$  as function of metallicity for all our target GCs, along with values from the literature for NGC 6752, M4, M5, and NGC 6388. We deliberately omitted data for  $\omega$  Centauri and NGC 3201 because of the non-standard nature of these systems. In fact,  $\omega$  Centauri is known to host extremely large variations in metallicity and  $s$ -process elements (Marino et al. 2011b) and has been suggested to be the nucleus of a disrupted dwarf galaxy, while recently Simmerer et al. (2013) questioned the mono-metallic nature of NGC 3201. The first key feature evident in Figure 3 is that GCs exhibit solar or even slightly sub-solar  $[\text{Rb}/\text{Fe}]$  ratios, with the exception of M4. The unusually high intrinsic  $s$ -process-element content of M4 has been the subject of

<sup>10</sup> Milone et al. (2012) identified a multiple sub-giant branch (SGB) in 47 Tuc; the faint SGB might be characterised by different  $s$ -process element abundances (including Rb), however, it accounts only for a very small fraction of the GC population and its progeny could not have been targeted here. A dedicated investigation is needed to ascertain its heavy-element content; it is worth mentioning in this context that Marino (2013) detected a significant N enhancement in the faint SGB of this cluster.

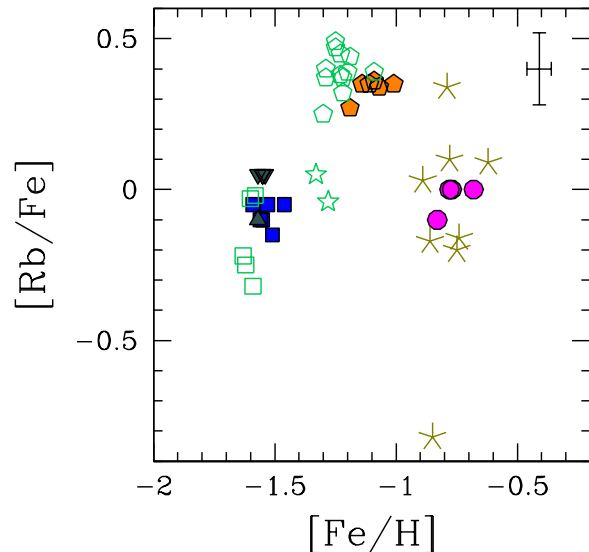


Fig. 3.—  $[\text{Rb}/\text{Fe}]$  versus  $[\text{Fe}/\text{H}]$  for our sample clusters (squares, triangles—upside down for upper limits—, and circles are for NGC 6752, NGC 1904, and 47 Tuc respectively) along with data for M4 (filled and empty pentagons are stars from D’Orazi et al. 2013 and Yong et al. 2008b, respectively), M5 (starred symbols; Yong et al. 2008b), NGC 6752 (open squares; Yong et al. 2006), and NGC 6388 (asterisks; Wallerstein et al. 2007). A representative errorbar is shown in the upper-right corner.

many observational studies based on first-peak and second-peak  $s$ -process elements (e.g., Ivans et al. 1999; Yong et al. 2008a; D’Orazi et al. 2013a) and is thought to reflect a distinct formation and pristine chemical enrichment. The second key feature in Figure 3 is that *none of the clusters, except for NGC 6388, display an internal variation in their Rb content, within the uncertainties.* This constant roughly solar Rb abundance exhibited by GCs represent a crucial result considering the large range in metallicity and global structural parameters encompassed. Importantly for the internal pollution scenario this also implies that the p-capture element variations detected in all Galactic GCs are *not* accompanied by a similar trend in the Rb abundances. This can be seen clearly in Figure 4 where the  $[\text{Rb}/\text{Fe}]$  ratios are plotted as a function of Na and O abundances: internal spreads of 0.3–0.7 dex (depending on the GC) in Na and of 0.2–0.6 dex in O are not accompanied by changes in Rb.

Only in NGC 6388 large Rb variations appear to be present. Wallerstein et al. (2007) measured a mean value of  $[\text{Rb}/\text{Fe}] = -0.10 \pm 0.12$  (rms=0.34), with one star (#91) showing an extremely low Rb abundance (i.e.,  $[\text{Rb}/\text{Fe}] = -0.82$ ). However, if we do not take into account this star (as these authors do in the computation of the mean light  $s$ -process element abundances), the average results in  $[\text{Rb}/\text{Fe}] = 0.00 \pm 0.07$  (rms=0.20). Wallerstein et al. (2007) call the attention on two stars in their sample, #91 and #361, with very similar atmospheric parameters, but almost an order of magnitude different Rb abundances ( $[\text{Rb}/\text{Fe}] = -0.82$  dex and  $[\text{Rb}/\text{Fe}] = 0.09$ , respectively). Interestingly, the two stars are also characterised by Na and Al abundances correlated with Rb:  $[\text{Na}/\text{Fe}] = -0.07$  and  $[\text{Al}/\text{Fe}] = -0.26$  for star #91 and  $[\text{Na}/\text{Fe}] = 0.47$  and  $[\text{Al}/\text{Fe}] = 0.53$  for star #361. Considering all the data from Wallerstein et al. (2007), Figure 3 shows that there is a positive correlation between the Rb and Na and Al

abundances, however, such a correlation disappears if star #91 is discarded, and a Rb - O anticorrelation is also not present at any statistically significant level. Furthermore, the [Rb/H] ratios derived by Wallerstein et al. (2007) do not exhibit any correlation with their [Zr/H] values. Since the Rb uncertainties quoted by Wallerstein et al. (2007) are  $\sim 0.3$  dex (as given by the rms of the mean Rb abundances from the two Rb  $\gamma$  resonance lines) and their sample stars are characterised by temperatures notably cooler (down to  $T_{\text{eff}}=3500\text{K}$ ) than those analysed in all the other studies discussed here, new measurements of Rb and other  $s$ -process elements in NGC 6388 are mandatory before any firm conclusion can be drawn on the presence (or lack) of an internal spread of Rb in this GC.

#### 4. DISCUSSION

Our finding provides a strong constraint on the internal pollution scenario for GCs. The observed lack of a correlation between Rb and p-capture elements, if confirmed also for NGC 6388, may be used as an argument against IM-AGB stars as the polluters because extremely high Rb overabundances (up to 2.6 dex) are observed in IM-AGB stars in the Galaxy (García-Hernández et al. 2006) and even higher values (up to 5 dex) are seen in IM-AGB stars in the Large and Small Magellanic Clouds (LMC and SMC, respectively, García-Hernández et al. 2009). This is qualitatively in agreement with theoretical models, which predict that IM-AGB stars synthesise and eject substantial amounts of Rb due to the high neutron density reached during the activation of the  $^{22}\text{Ne}(\alpha, n)^{25}\text{Mg}$  reaction (van Raai et al. 2012).

Interestingly, the IM-AGB observational trends of [Rb/Fe] increasing with increasing the stellar mass and with decreasing the metallicity are well explained by the models (van Raai et al. 2012) while the observed absolute [Rb/Fe] abundances are much higher than predicted. Karakas et al. (2012) demonstrated that, for solar-metallicity stars, [Rb/Fe] $\sim 1.4$  could be reached if the final stage of mass-loss was delayed resulting in a larger number of thermal pulses and increased Rb production. However, a most irksome problem is that the observed [Zr/Fe] are roughly solar (within 0.5 dex, García-Hernández et al. 2007), suggesting no production of this element in IM-AGB stars<sup>11</sup>. This results in [Rb/Zr] ratios much higher than the maximum of  $\approx 0.5$  dex allowed by the  $s$ -process, considering that the four elements Rb, Sr, Y, and Zr belong to the first  $s$ -process peak defined by a magic number of neutrons of 50 and are produced in similar abundances (within a factor of  $\sim 3$ ) for any given total time-integrated neutron flux. As discussed in detail by García-Hernández et al. (2009) and van Raai et al. (2012), there are many difficulties in obtaining reliable quantitative abundances in IM-AGB stars due to the modelling of the complex, pulsating, dusty atmospheres of these stars. New model atmospheres are currently being developed (A. García-Hernández, private communication) which may help to shed light on this problem.

In relation to GCs, if Rb production in fact occurs in IM-AGB stars at the level seen in the MCs and if the ejecta of these stars contribute to the formation of the SG, we should find trace of the presence of Rb, particularly in clusters of similar metallicity as the MCs. The determination of the Rb abundances in 47 Tuc and NGC 6388 is crucial in this respect

<sup>11</sup> In agreement with observations of roughly solar Se and Kr abundances (also within roughly 0.5 dex) in planetary nebulae of Type II, believed to be the progeny of IM-AGB stars (Sterling & Dinerstein 2008, Karakas et al. 2009).

because these clusters have approximately the same metallicity of the SMC ([Fe/H]  $\approx -0.7$  dex).

If the lack of a correlation between Rb and Na will be confirmed also for NGC 6388, we are in the presence of a conundrum to which possible solutions are:

- the mass range of the stars that produce Rb does not play a role in GCs, i.e., the IM-AGB polluters could be on average of mass lower or higher (i.e., Super-AGBs, as suggested by Garcia-Hernandez et al. 2013) than the IM-AGB stars observed in the MCs;
- the mass-loss rate of IM-AGB stars is fast (Ventura & D'Antona 2005), resulting in a small number of thermal pulses and insignificant  $s$ -process enhancements (D'Orazi et al. 2013a). Because this solution is the opposite of that proposed by Karakas et al. (2012) to explain the [Rb/Fe] observations in IM-AGB stars, it would call for a different evolution of IM-AGB stars in the cluster environment as compared to the field.
- Alternatively, if updated models of the atmospheres of IM-AGB stars result in a revision of the [Rb/Fe] ratios in the MCs to much lower values, then low-metallicity IM-AGB stars must experience a strong mass loss (see also the recent paper by Noel et al. 2013). In this case they would avoid significant production of  $s$ -process elements.
- Finally, it may be that the huge Rb production observed in the Rb-rich IM-AGB stars is related to the very final phase of the IM-AGB phase, when most of the stellar mass has been already lost to the surroundings via stellar winds. In this case, the observed Rb abundances would be a signature present only in a small remnant envelope mass, rather than the overall yield over the whole lifetime of the star. We note that all the Rb-rich stars observed stars are heavily obscured, i.e., at the end of their evolution, while massive AGB stars at the beginning of the AGB phase are super Li-rich and show no Rb enhancement (García-Hernández et al. 2013).

#### 5. CONCLUDING REMARKS

Our study on Rb abundances in NGC 1904, NGC 6752, and 47 Tuc suggests that, at odds with p-capture elements, this element does not exhibit any internal variation beyond that expected from observational uncertainties. This behaviour appears to be true for clusters over a wide range of metallicity, however, it urgently needs to be confirmed, or disproved, for the high-metallicity GC NGC 6388. If the lack of internal variations is confirmed, the internal polluters responsible for the light-element spreads must not have produced *any*  $s$ -process elements to a significant extent. Obviously the opposite requirement has to be satisfied by the stellar sources responsible for  $s$ -process variations in “non-standard” GCs such as M22 (Marino et al. 2009), NGC 1851 (Yong & Grundahl 2008),  $\omega$  Centauri (Johnson & Pilachowski 2010; Marino et al. 2011b; D'Orazi et al. 2011), which implies that the type of stars that produced the Na-O anticorrelation in all GCs cannot be the same as those that produced the variations in  $s$ -process

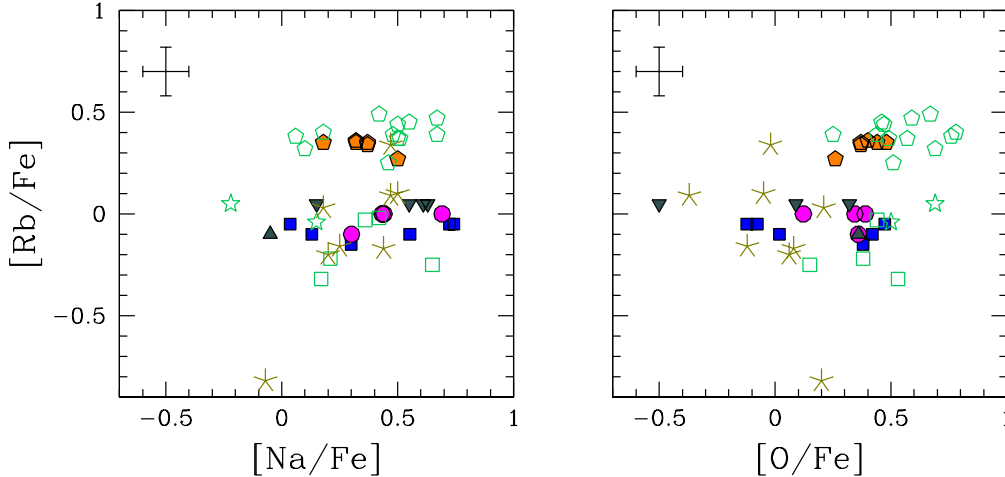


FIG. 4.— Run of Rb with p-capture elements Na and O. Symbols as for Figure 3. Na and O abundances are from Carretta et al. (2007, 2009b), Marino et al. (2008), Yong et al. (2003), Wallerstein et al. (2007).

elements detected in a small sub-sample of GCs (e.g.,  $\omega$  Cen, M22, NGC 1851).

Comparison with direct observations of Rb in IM-AGB stars in the MCs, i.e., close to the metallicity of 47 Tuc and NGC 6388, appears to indicate that IM-AGB stars should produce large amounts of Rb, in which case IM-AGB stars might be ruled out as candidates for the internal pollution scenario. On the other hand, the FRMS scenario does not face this problem as the winds of these stars during the main-sequence phase do not carry any *s*-process-elements enhancements (see the Introduction). However, these candidates face even bigger issues such as destruction/production of Li, no depletion in Mg, low fraction of SG stars, and close superimposition with core-collapse supernova timescales.

In conclusion, while the AGB framework has to face major challenges (not only limited to Rb) in reproducing the observed features of GCs, we still consider it as the most promising scenario and propose a number of possible solutions to solve the possible Rb conundrum in the IM-AGB stars scenario, such as e.g., a different mass range of the AGB polluters, a different IM-AGB mass-loss rate

(Ventura & D’Antona 2005; D’Orazi et al. 2013a), or the Rb production being limited to the very final thermal pulses. It should also be kept in mind that the observed [Rb/Zr] ratios are currently orders of magnitude higher than values predicted by *s*-process models and might be revised in light of the many uncertainties in the model atmospheres of AGB stars (García-Hernández et al. 2009). Finally, we urgently call for new, dedicated observations of NGC 6388 to clarify the current picture. Also, future observations of metal-rich clusters where a large helium difference between the FG and the SG is well known (e.g., NGC 6441) will help in putting much stronger constraint on dilution and a more accurate estimate of the Rb abundance allowed to be produced by the polluters.

This work made extensive use of SIMBAD, VizieR, and NASA-ADS databases. VD is an ARC Super Science Fellow. ML is an ARC Future fellow and Monash fellow. SWC is supported by an ARC Discovery Project grant (DP1095368). We thank the referee for a very careful reading of the manuscript and for valuable and helpful comments and suggestions.

#### REFERENCES

- Abia, C., Busso, M., Gallino, R., et al. 2001, *ApJ*, 559, 1117  
 Alves-Brito, A., Yong, D., Meléndez, J., Vásquez, S., & Karakas, A. I. 2012, *A&A*, 540, A3  
 Alves-Brito, A., Barbuy, B., Ortolani, S., et al. 2005, *A&A*, 435, 657  
 Anderson, J., Piotto, G., King, I. R., Bedin, L. R., & Guhathakurta, P. 2009, *ApJ*, 697, L58  
 Arlandini, C., Käppeler, F., Wisshak, K., et al. 1999, *ApJ*, 525, 886  
 Armosky, B. J., Sneden, C., Langer, G. E., & Kraft, R. P. 1994, *AJ*, 108, 1364  
 Bragaglia, A., Gratton, R. G., Carretta, E., et al. 2012, *A&A*, 548, A122  
 Busso, M., Lambert, D. L., Beglio, L., et al. 1995, *ApJ*, 446, 775  
 Carretta, E., Bragaglia, A., Gratton, R., & Lucatello, S. 2009a, *A&A*, 505, 139  
 Carretta, E., Bragaglia, A., Gratton, R. G., Lucatello, S., & Momany, Y. 2007, *A&A*, 464, 927  
 Carretta, E., Bragaglia, A., Gratton, R. G., et al. 2010, *A&A*, 516, A55  
 Carretta, E., Gratton, R. G., Bragaglia, A., D’Orazi, V., & Lucatello, S. 2013, *A&A*, 550, A34  
 Carretta, E., Lucatello, S., Gratton, R. G., Bragaglia, A., & D’Orazi, V. 2011, *A&A*, 533, A69  
 Carretta, E., Bragaglia, A., Gratton, R. G., et al. 2009b, *A&A*, 505, 117  
 Cohen, J. G. 1999, *AJ*, 117, 2434  
 de Laverny, P., & Recio-Blanco, A. 2013, *ArXiv e-prints*, arXiv:1306.4528  
 de Mink, S. E., Pols, O. R., Langer, N., & Izzard, R. G. 2009, *A&A*, 507, L1  
 Decressin, T., Charbonnel, C., & Meynet, G. 2007, *A&A*, 475, 859  
 D’Ercole, A., D’Antona, F., Carini, R., Vesperini, E., & Ventura, P. 2012, *MNRAS*, 423, 1521  
 D’Orazi, V., Campbell, S. W., Lugaro, M., et al. 2013a, *MNRAS*, 433, 366  
 D’Orazi, V., Gratton, R., Lucatello, S., et al. 2010, *ApJ*, 719, L213  
 D’Orazi, V., Gratton, R. G., Pancino, E., et al. 2011, *A&A*, 534, A29  
 D’Orazi, V., & Marino, A. F. 2010, *ApJ*, 716, L166  
 D’Orazi, V., Lucatello, S., Lugaro, M., et al. 2013b, *ApJ*, 763, 22  
 François, P. 1991, *A&A*, 247, 56  
 Frischknecht, U., Hirschi, R., & Thielemann, F.-K. 2012, *A&A*, 538, L2  
 Gallino, R., Arlandini, C., Busso, M., et al. 1998, *ApJ*, 497, 388  
 García-Hernández, D. A., García-Lario, P., Plez, B., et al. 2006, *Science*, 314, 1751  
 —. 2007, *A&A*, 462, 711  
 García-Hernández, D. A., Karakas, A. I., & Lugaro, M. 2013, *ArXiv e-prints*, arXiv:1301.1492  
 García-Hernández, D. A., Zamora, O., Yagüe, A., et al. 2013, *A&A*, 555, L3  
 García-Hernández, D. A., Machado, A., Lambert, D. L., et al. 2009, *ApJ*, 705, L31  
 Gonzalez, G., & Wallerstein, G. 1998, *AJ*, 116, 765  
 Goriely, S. 1999, *A&A*, 342, 881  
 Gratton, R. G., Carretta, E., & Bragaglia, A. 2012, *A&A Rev.*, 20, 50  
 Gratton, R. G., Lucatello, S., Carretta, E., et al. 2011, *A&A*, 534, A123  
 Harris, W. E. 1996, *VizieR Online Data Catalog*, 7195, 0  
 Heil, M., Käppeler, F., Uberseder, E., et al. 2008, *Phys. Rev. C*, 78, 025802  
 Ivans, I. I., Sneden, C., Kraft, R. P., et al. 1999, *AJ*, 118, 1273

- James, G., François, P., Bonifacio, P., et al. 2004, *A&A*, 427, 825
- Johnson, C. I., & Pilachowski, C. A. 2010, *ApJ*, 722, 1373
- Karakas, A. I., García-Hernández, D. A., & Lugaro, M. 2012, *ApJ*, 751, 8
- Karakas, A. I., van Raai, M. A., Lugaro, M., Sterling, N. C., & Dinerstein, H. L. 2009, *ApJ*, 690, 1130
- Kurucz, R. 1993, *ATLAS9 Stellar Atmosphere Programs and 2 km/s grid*. Kurucz CD-ROM No. 13. Cambridge, Mass.: Smithsonian Astrophysical Observatory, 1993., 13
- Lambert, D. L., & Luck, R. E. 1976, *The Observatory*, 96, 100
- Lind, K., Charbonnel, C., Decressin, T., et al. 2011, *A&A*, 527, A148
- Maccarone, T. J., & Zurek, D. R. 2012, *MNRAS*, 423, 2
- Marino, A. F. 2013, *Mem. Soc. Astron. Italiana*, 84, 29
- Marino, A. F., Milone, A. P., Piotto, G., et al. 2009, *A&A*, 505, 1099
- Marino, A. F., Villanova, S., Milone, A. P., et al. 2011a, *ApJ*, 730, L16
- Marino, A. F., Villanova, S., Piotto, G., et al. 2008, *A&A*, 490, 625
- Marino, A. F., Milone, A. P., Piotto, G., et al. 2011b, *ApJ*, 731, 64
- Milone, A. P., Piotto, G., Bedin, L. R., et al. 2012, *ApJ*, 744, 58
- Milone, A. P., Marino, A. F., Piotto, G., et al. 2013, *ApJ*, 767, 120
- Monelli, M., Milone, A. P., Stetson, P. B., et al. 2013, *MNRAS*, 431, 2126
- Mucciarelli, A., Salaris, M., Lovisi, L., et al. 2011, *MNRAS*, 412, 81
- Noel, N. E. D., Greggio, L., Renzini, A., Carollo, M., & Maraston, C. 2013, *ArXiv e-prints*, arXiv:1305.3617
- Pasquini, L., Bonifacio, P., Molaro, P., et al. 2005, *A&A*, 441, 549
- Pasquini, L., Avila, G., Blecha, A., et al. 2002, *The Messenger*, 110, 1
- Pignatari, M., Gallino, R., Meynet, G., et al. 2008, *ApJ*, 687, L95
- Piotto, G. 2009, in *IAU Symposium*, Vol. 258, *IAU Symposium*, ed. E. E. Mamajek, D. R. Soderblom, & R. F. G. Wyse, 233–244
- Shen, Z.-X., Bonifacio, P., Pasquini, L., & Zaggia, S. 2010, *A&A*, 524, L2
- Simmerer, J., Ivans, I. I., Filler, D., et al. 2013, *ApJ*, 764, L7
- Smith, G. H. 2008, *PASP*, 120, 952
- Smith, V. V., Cunha, K., Ivans, I. I., et al. 2005, *ApJ*, 633, 392
- Smith, V. V., Suntzeff, N. B., Cunha, K., et al. 2000, *AJ*, 119, 1239
- Snedden, C. A. 1973, PhD thesis, THE UNIVERSITY OF TEXAS AT AUSTIN.
- Sterling, N. C., & Dinerstein, H. L. 2008, *ApJS*, 174, 158
- Tomkin, J., & Lambert, D. L. 1999, *ApJ*, 523, 234
- van Raai, M. A., Lugaro, M., Karakas, A. I., García-Hernández, D. A., & Yong, D. 2012, *A&A*, 540, A44
- Ventura, P., & D'Antona, F. 2005, *A&A*, 439, 1075
- . 2009, *A&A*, 499, 835
- . 2011, *MNRAS*, 410, 2760
- Ventura, P., D'Antona, F., Mazzitelli, I., & Gratton, R. 2001, *ApJ*, 550, L65
- Villanova, S., Geisler, D., & Piotto, G. 2010, *ApJ*, 722, L18
- Wallerstein, G., Kovtyukh, V. V., & Andrievsky, S. M. 2007, *AJ*, 133, 1373
- Worley, C. C., Cottrell, P. L., McDonald, I., & van Loon, J. T. 2010, *MNRAS*, 402, 2060
- Yong, D., Aoki, W., Lambert, D. L., & Paulson, D. B. 2006, *ApJ*, 639, 918
- Yong, D., & Grundahl, F. 2008, *ApJ*, 672, L29
- Yong, D., Grundahl, F., Lambert, D. L., Nissen, P. E., & Shetrone, M. D. 2003, *A&A*, 402, 985
- Yong, D., Grundahl, F., Nissen, P. E., Jensen, H. R., & Lambert, D. L. 2005, *A&A*, 438, 875
- Yong, D., Karakas, A. I., Lambert, D. L., Chieffi, A., & Limongi, M. 2008a, *ApJ*, 689, 1031
- Yong, D., Lambert, D. L., Paulson, D. B., & Carney, B. W. 2008b, *ApJ*, 673, 854
- Yong, D., Meléndez, J., Cunha, K., et al. 2008c, *ApJ*, 689, 1020